THE ROLE OF MODEL FIDELITY IN MODEL PREDICTIVE CONTROL BASED HAZARD AVOIDANCE IN UNMANNED GROUND VEHICLES USING LIDAR SENSORS

Jiechao Liu
Mechanical Engineering
University of Michigan
Ann Arbor, MI 48109
ljch@umich.edu

Paramsothy Jayakumar
U.S. Army RDECOM-TARDEC
Warren, MI 48397
paramsothy.jayakumar.civ@mail.mil

James L. Overholt
U.S. Army RDECOM-TARDEC
Warren, MI 48397
james.l.overholt2.civ@mail.mil

Jeffrey L. Stein
Mechanical Engineering
University of Michigan
Ann Arbor, MI 48109
stein@umich.edu

Tulga Ersal
Mechanical Engineering
University of Michigan
Ann Arbor, MI 48109
tersal@umich.edu

ABSTRACT

Unmanned ground vehicles (UGVs) are gaining importance and finding increased utility in both military and commercial applications. Although earlier UGV platforms were typically exclusively small ground robots, recent efforts started targeting passenger vehicle and larger size platforms. Due to their size and speed, these platforms have significantly different dynamics than small robots, and therefore the existing hazard avoidance algorithms, which were developed for small robots, may not deliver the desired performance. The goal of this paper is to present the first steps towards a model predictive control (MPC) based hazard avoidance algorithm for large UGVs that accounts for the vehicle dynamics through high fidelity models and uses only local information about the environment as provided by the onboard sensors. Specifically, the paper presents the MPC formulation for hazard avoidance using a light detection and ranging (LIDAR) sensor and applies it to a case study to investigate the impact of model fidelity on the performance of the algorithm, where performance is measured mainly by the time to reach the target point. Towards this end, the case study compares a 2 degrees-of-freedom (DoF) vehicle dynamics representation to a 14 DoF representation as the model used in MPC. The results show that the 2 DoF model can perform comparable to the 14 DoF model if the safe steering range is established using the 14 DoF model rather than the 2 DoF model itself. The conclusion is that high fidelity models are needed to push autonomous vehicles to their limits to increase their performance, but simulating the high fidelity models online within the MPC may not be as critical as using them to establish the safe control input limits.

INTRODUCTION

Unmanned ground vehicles (UGVs) hold great potential for increased safety, performance, and convenience, and are therefore attracting interest for both commercial and military applications. Small ground robots that are either teleoperated or semi or fully autonomous are already in use. Currently, particular interest is in autonomous UGVs that are at least the size of a passenger vehicle. In the commercial field, almost all major automakers and even companies from other sectors are pursuing autonomous passenger vehicles [1]. As a military example, the Autonomous Platform Demonstrator (APD) is a 9.3 ton vehicle that has been used to develop, integrate, and test many next generation UGV mobility technologies such as hybrid electric drive systems, advanced suspension systems, thermal management systems, and UGV safety systems [2]. It is capable of reaching speeds up to 50 miles per hour (22.35 m/s) and performing maneuvers at those speeds [2].

One important problem in autonomous UGVs regardless of their size is hazard avoidance, which refers to the problem of safely maneuvering around obstacles while traveling to a target point. Many hazard avoidance algorithms have been developed in the literature that allow for fast, continuous, and smooth motion of the UGV among unexpected obstacles [3]. These algorithms generate a hazard-avoiding action in response to online sensor signals. Some early examples include the artificial potential field method [4, 5], the vector field

Report Documentation Page

Form Approved
OMB No. 0704-0188

1. REPORT DATE	2. REPORT TYPE	3. DATES COVERED
08 MAR 2013	**Journal Article**	**05-10-2012 to 28-01-2013**

4. TITLE AND SUBTITLE
THE ROLE OF MODEL FIDELITY IN MODEL PREDICTIVE CONTROL BASED HAZARD AVOIDANCE IN UNMANNED GROUND VEHICLES USING LIDAR SENSORS

5a. CONTRACT NUMBER

5b. GRANT NUMBER

5c. PROGRAM ELEMENT NUMBER

6. AUTHOR(S)
Jiechao Liu; Paramsothy Jayakumar; James Overholt; Jeffrey Stein; Tulga Ersal

5d. PROJECT NUMBER

5e. TASK NUMBER

5f. WORK UNIT NUMBER

7. PERFORMING ORGANIZATION NAME(S) AND ADDRESS(ES)
Mechanical Engineering,University of Michigan,Ann Arbor,Mi,48109

8. PERFORMING ORGANIZATION REPORT NUMBER
; #23704

9. SPONSORING/MONITORING AGENCY NAME(S) AND ADDRESS(ES)
U.S. Army TARDEC, 6501 East Eleven Mile Rd, Warren, Mi, 48397-5000

10. SPONSOR/MONITOR'S ACRONYM(S)
TARDEC

11. SPONSOR/MONITOR'S REPORT NUMBER(S)
#23704

12. DISTRIBUTION/AVAILABILITY STATEMENT
Approved for public release; distribution unlimited

13. SUPPLEMENTARY NOTES
Submitted to Dynamic Systems and Control Conference 2013

14. ABSTRACT

Unmanned ground vehicles (UGVs) are gaining importance and finding increased utility in both military and commercial applications. Although earlier UGV platforms were typically exclusively small ground robots, recent efforts started targeting passenger vehicle and larger size platforms. Due to their size and speed, these platforms have significantly different dynamics than small robots, and therefore the existing hazard avoidance algorithms, which were developed for small robots, may not deliver the desired performance. The goal of this paper is to present the first steps towards a model predictive control (MPC) based hazard avoidance algorithm for large UGVs that accounts for the vehicle dynamics through high fidelity models and uses only local information about the environment as provided by the onboard sensors. Specifically, the paper presents the MPC formulation for hazard avoidance using a light detection and ranging (LIDAR) sensor and applies it to a case study to investigate the impact of model fidelity on theperformance of the algorithm, where performance is measured mainly by the time to reach the target point. Towards this end, the case study compares a 2 degrees-of-freedom (DoF) vehicle dynamics representation to a 14 DoF representation as the model used in MPC. The results show that the 2 DoF model can perform comparable to the 14 DoF model if the safe steering range is established using the 14 DoF model rather than the 2 DoF model itself. The conclusion is that high fidelity models are needed to push autonomous vehicles to their limits to increase their performance, but simulating the high fidelity models online within the MPC may not be as critical as using them to establish the safe control input limits.

15. SUBJECT TERMS

16. SECURITY CLASSIFICATION OF:			17. LIMITATION OF ABSTRACT	18. NUMBER OF PAGES	19a. NAME OF RESPONSIBLE PERSON
a. REPORT **unclassified**	b. ABSTRACT **unclassified**	c. THIS PAGE **unclassified**	**Public Release**	**10**	

Standard Form 298 (Rev. 8-98)
Prescribed by ANSI Std Z39-18

histogram method [3, 6-10], and the dynamic window approach [11, 12]. However, these algorithms typically focus on small ground robots and hence rely on assumptions such as representing the vehicle as a point, which do not hold for larger UGVs. Thus, hazard avoidance algorithms developed for small UGVs may not deliver the desired performance in larger UGVs.

More recent work aimed to improve the algorithms originally developed for small robots and to adapt them to large, high-speed UGVs. For example, Shimoda et al. [5] used trajectory space based potential field method to navigate a high speed UGV on rough terrain, avoiding discrete static hazards and dynamically inadmissible maneuvers. A potential field is constructed in the trajectory space, which is a two-dimensional space of a UGV's instantaneous path curvature and longitudinal velocity, and vehicle maneuvers are selected based on the properties of the field. The potential field is defined as a sum of potential functions relating to the waypoint location, desired velocity, hazard, rollover and side slip constraints. Although computationally efficient, this method does not guarantee feasibility or optimality [13].

To address the optimality problem, more rigorous methods have been pursued leveraging the model predictive control (MPC) approach. MPC is a form of control in which the current control action is obtained by solving a finite horizon open-loop optimal control problem using the current state of the plant as the initial state; the optimization yields an optimal control sequence and the first control in this sequence is applied to the plant. MPC is a promising approach for hazard avoidance due to its capability to handle input saturation, system nonlinearity, and state constraints in a dynamic environment. For example, Tahirovic and Magnani [14] provided a framework for incorporating a vehicle model into navigation by using an adapted version of passivity-based nonlinear model predictive control to extend the convergent dynamic window approach [12]. It can be considered a generalized navigation planning technique able to include the high fidelity models required to describe the dynamics of vehicles moving outdoor on rough terrain.

Even though this work and several others [15-17] demonstrated successful application of MPC to hazard avoidance, several research questions still remain to be addressed. For example, the passivity-based MPC navigation algorithm assumes the environment is completely known. In reality, only local information from onboard sensors will be available. Furthermore, to reduce the computational load, only simple vehicle dynamics models such as the 2 degrees of freedom (DoF) representation have been considered so far as the model in MPC. As pointed by Park [15], only when the assumptions used to derive the simplified model are satisfied, the actual vehicle can track the generated trajectory based on this simplified model. The level of complexity of the model that needs to be used in MPC for best performance is unknown.

Therefore, the goal of this paper is twofold: (1) to describe an MPC based hazard avoidance algorithm that works only with local information about the environment from the onboard sensors; and (2) to evaluate on a case study the performance of the algorithm with low versus high fidelity vehicle models. A typical 4-wheel truck is considered as an example vehicle platform. Regarding the first goal, the vehicle is assumed to be equipped with a light detection and ranging (LIDAR) sensor. Regarding the second goal, the performance is mainly measured by the time to reach the target; the best performance is achieved when the vehicle reaches the target safely and in minimum time. Two different representations of vehicle dynamics within MPC are compared; a 2 DoF representation as a lower fidelity model and a 14 DoF representation as a higher fidelity model.

Throughout the paper it is assumed that the computational power needed for using high fidelity models within MPC can be met in real time by leveraging the recent developments in high power computing capabilities [18]. Thus, computational aspects of the algorithm are not discussed and computational time is not used as a performance metric.

The rest of the paper is organized as follows. First, the MPC based hazard avoidance algorithm is presented. The vehicle models, constraints, cost function, and dynamic optimizer are described in detail. Simulation results are presented next using two different obstacle maps to validate the proposed approach and evaluate its performance with 2 DoF versus 14 DoF model in the MPC. Finally, the limitations of this study are outlined to guide future research and conclusions are drawn.

MPC-BASED HAZARD AVOIDANCE

The basic principle of MPC is illustrated in Fig. 1. At time step k, starting from the sampled initial value, an optimal control input u is computed by solving an open-loop, constrained, finite-time optimal control problem for the prediction horizon p. The resulting estimated optimal output $\hat{y}$ satisfies the pre-defined constraints and minimizes a cost function. Only the first value of the computed control sequence is applied. Due to model simplifications, model parameter

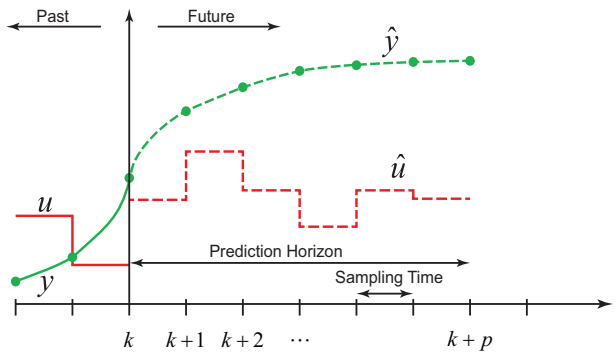

FIGURE 1. BASIC PRINCIPLE OF MPC

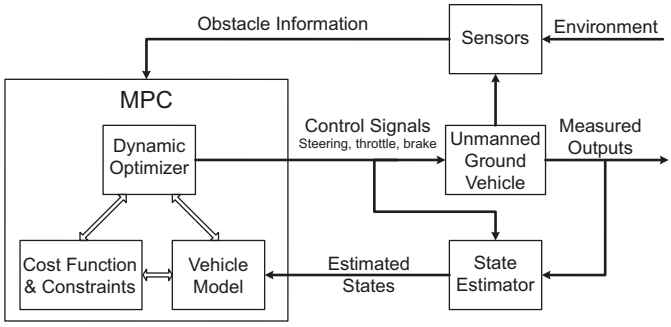

FIGURE 2. SCHEMATIC OF MPC-BASED HAZARD AVOIDANCE ALGORITHM

uncertainties, and/or other types of noise and uncertainties, the actual output y will be different from the predicted value. Therefore, at the next time step $k+1$, the optimal control problem is solved again over a shifted horizon based on the new state measurements. This process is thus iterated at each time step.

Figure 2 illustrates at a high level how MPC can be utilized for hazard avoidance purposes. The three main components of the MPC-based hazard avoidance algorithm are the vehicle model, the cost function and constraints, and the dynamic optimizer. These components will be discussed in detail below. The outputs of the hazard avoidance algorithm are the control signals for the UGV. In general, they are the steering wheel angle, throttle and brake pedal positions; however, for the purposes of this paper, it is assumed that the vehicle speed is constant and thus only the steering angle is considered as the control signal. The UGV will in reality be an actual vehicle platform; however, this work is simulation based and therefore the UGV is represented using a vehicle model, which will also be described below. The state estimator block is needed to estimate the full state of the vehicle from the control signals and measured outputs to be used as the initial condition for the vehicle model used in MPC. In this work, since the UGV is simulated, the full state information is available and hence the state estimator is not considered. Finally, the information about the environment is assumed to be obtained using a LIDAR.

The rest of this section describes the vehicle models, cost function and constraints, and the dynamic optimizer used in this work.

Vehicle Model

There are two places in the general schematic in Fig. 2 where a vehicle model is used in this work. To validate the hazard avoidance algorithm in simulation, a high-fidelity vehicle model is needed to represent the UGV. A 14 DoF representation is used for this purpose as a first step towards higher fidelity representations. In addition, a model of the vehicle is also needed in the MPC. Towards this end, this work considers two different representations: a 2 DoF model and the 14 DoF model. Both models are described next.

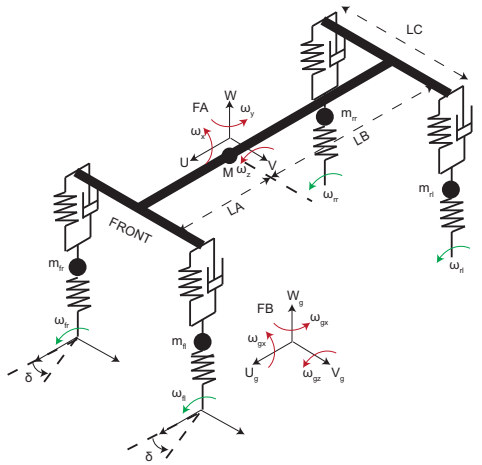

FIGURE 3. 14 DOF VEHICLE MODEL SCHEMATIC

The 14 DoF vehicle model, which consists of a single sprung mass connected to four unsprung masses, is implemented as shown in Fig. 3 [19]. The sprung mass is represented as a plane and is allowed to pitch, roll, and yaw, as well as displace in vertical, lateral and longitudinal directions. The unsprung masses are allowed to bounce vertically with respect to the sprung mass. Each wheel is also allowed to rotate along its horizontal axis and only the two front wheels are free to steer. In summary, this model consists of 6 DoF at the vehicle chassis center of gravity (CG), and 2 DoF at each of the four wheels, including vertical suspension travel and wheel spin.

To represent the tire traction forces, the lookup table based models used in TRUCKSIM [20] are adopted. Nonlinear tables are used to represent lateral forces and aligning moments as a function of slip angle and vertical load. Another nonlinear table is used to represent longitudinal forces as a function of slip ratio and vertical load. Two-dimensional linear data interpolation is used to determine the forces and moment for a specific combination of slip and load. Combined slip effects are not considered.

This vehicle model is parameterized for a typical 4 wheel

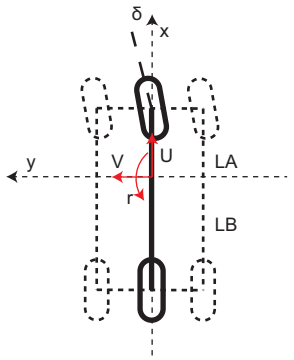

FIGURE 4. 2 DOF VEHICLE MODEL SCHEMATIC

truck and used in the simulation to represent the real system.

The standard vehicle model used in the state-of-the-art MPC-based hazard avoidance algorithms is a 2 DoF vehicle representation, with either assuming constant cornering stiffness or augmenting the vehicle model with Pacejka Magic Formula Tire Model [14-17]. Thus, as a baseline, a 2 DoF vehicle model is also used in this study with a constant cornering stiffness approach. The model is illustrated in Fig. 4.

The parameters of the 2 DoF and 14 DoF models are set identical except for the tire parameters. The 14 DoF is using a tire model as described above, whereas the 2 DoF model is using the constant cornering stiffness approach. To minimize the difference between the predictive capabilities of the two models, the cornering stiffnesses used in the 2 DoF model are tuned to match the response of the 2 and 14 DoF models as closely as possible. Figures 5 and 6 compare the vehicle trajectories and lateral accelerations, respectively, predicted by the two models under different steering conditions. The results confirm the finding in the literature that the 2 DoF starts losing its validity after a lateral acceleration of 0.5 g [15].

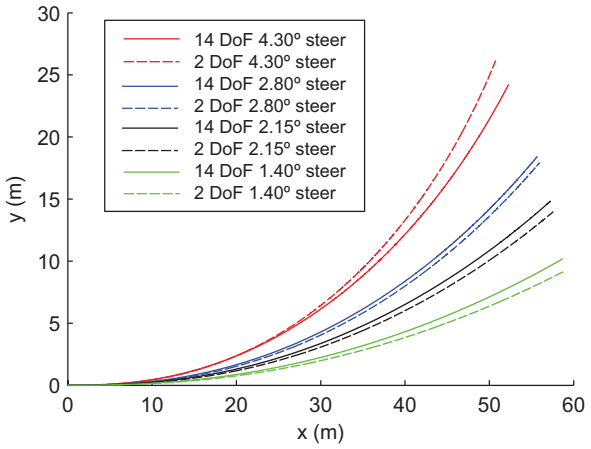

FIGURE 5. VEHICLE TRAJECTORIES FOR 20 M/S VELOCITY PREDICTED BY THE TWO MODELS

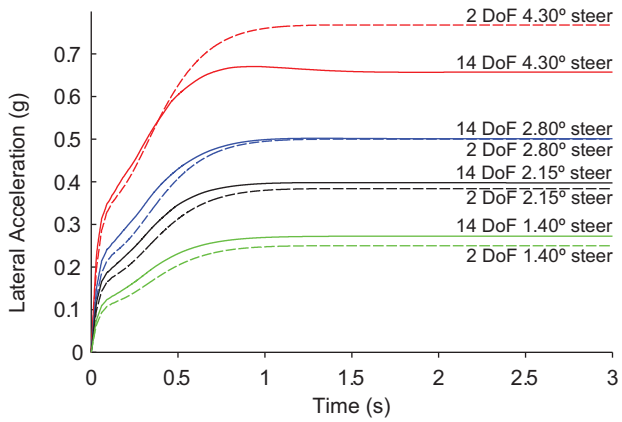

FIGURE 6. LATERAL ACCELERATIONS FOR 20 M/S VELOCITY PREDICTED BY THE TWO MODELS

Cost Function and Constraints

The cost function and constraints need to be specified to satisfy the objective of avoiding the locally detected obstacles while guaranteeing vehicle safety and minimizing the travel time. When the speed of the vehicle is constant as in this study, minimizing the travel time is the same as minimizing the travel distance.

Constraints. The constraints represent the hard requirements of avoiding collision and ensuring vehicle safety. These requirements are hard in the sense that their violation is not allowed under any circumstances.

To avoid collision with the obstacles, a minimum acceptable distance between the center of gravity of the vehicle and any detected points by the LIDAR sensor (i.e., the boundaries of the obstacles) is defined and set to 3 meters.

In this study, ensuring vehicle safety is translated to avoiding tire lift-off for the 14 DoF model. This is a conservative criterion used to prevent rollover [21]. It is also part of the vehicle acceptability tests used in the military. Note that the roll angle or lateral acceleration threshold can also be used to define the safety of a vehicle [22, 23]. Since the 2 DoF cannot predict tire lift-off, a maximum lateral acceleration of 0.5 g, i.e., the model's reported range of validity [15], is used as the safety limit for the 2 DoF model.

As shown in Fig. 7, for the 14 DoF model traveling at a constant speed, when the steering angle increases, the vertical tire force of one of the tires becomes smaller. Hence, there exists a maximum steering angle such that the minimum vertical tire force is close to zero (4.3° in the example shown). When the steering angle increases by 0.1°, tire lift-off is observed (4.4° in the example shown).

Similarly, the maximum allowable lateral acceleration

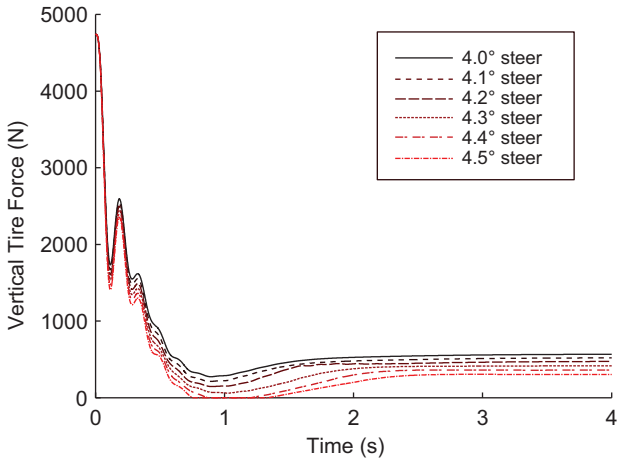

FIGURE 7. VERTICAL TIRE FORCE FOR VARIOUS STEERING COMMANDS AT 20 M/S FOR THE 14 DOF MODEL

places an upper limit to the steering angle in the 2 DoF model. Figure 8 illustrates how lateral acceleration increases with steering angle.

Note that the maximum steering angle is a function of vehicle speed. There exist other factors that can change the maximum steering angle, for example, the slope of the terrain. However, in this study, the vehicle is assumed to move on a constant friction flat surface. Therefore, the maximum steering angle is only a function vehicle speed. For speeds ranging from 10 m/s to 30 m/s, the relationship between the maximum steering angle and the speed is shown in Fig. 9 for both the 2 DoF and 14 DoF models. This also corresponds to a minimum turning radius as shown in Fig. 10.

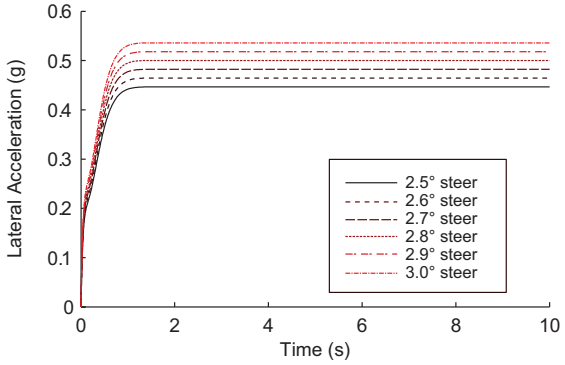

FIGURE 8. LATERAL ACCELERATION FOR VARIOUS STEERING COMMANDS AT 20 M/S FOR THE 2 DOF MODEL

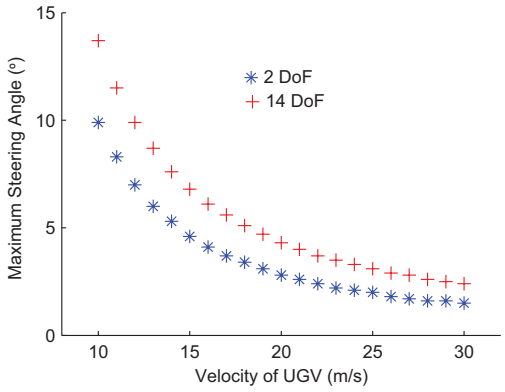

FIGURE 9. MAXIMUM STEERING ANGLE AS A FUNCTION OF SPEED

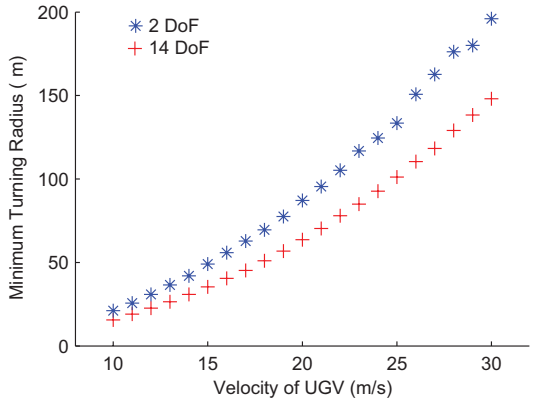

FIGURE 10. MINIMUM TURNING RADIUS AS A FUNCTION OF SPEED

In summary, the two hard requirements considered in this work are maneuvering without collision and without tire lift-off (14 DoF) or excessive lateral acceleration (2 DoF). For the first requirement, obstacle information from the LIDAR is used. The minimum acceptable distance between the center of gravity of the vehicle and obstacles is set to 3 meters. For the second requirement, if the steer angle is below the maximum allowable value at a given speed, the safety of the vehicle can be guaranteed when the vehicle moves on a constant friction flat surface. Hence, the search space for the steering angle is limited to the feasible space.

These hard requirements are implemented as hard constraints in the sense that if a control input sequence is predicted to cause any constraint violation, it will not be considered as a candidate.

Cost Function. The cost function defines the soft requirement; i.e., in what sense the trajectory is optimal. Two terms are included in the current formulation as follows

$$J = d_g\left(t_0 + nT\right) + w\alpha\left(t_0 + nT\right)$$

where

$$d_g\left(t_0 + nT\right) = \sqrt{\left(x\left(t_0 + nT\right) - x_g\right)^2 + \left(y\left(t_0 + nT\right) - y_g\right)^2}$$

$$\alpha\left(t_0 + nT\right) = \tan^{-1}\left(\frac{y_g - y\left(t_0 + nT\right)}{x_g - x\left(t_0 + nT\right)}\right)$$

with t_0 representing the initial time, n the number of prediction steps, T the sampling time, x and y the position of the UGV, and x_g and y_g the position of the goal.

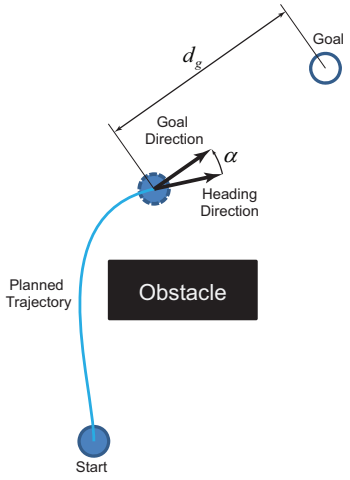

FIGURE 11. THE COMPONENTS OF THE COST FUNCTION

The first term encourages a shorter distance between the end of prediction horizon and the goal. Due to the constant speed assumption in this work, this term also aims to minimize the remaining travel time. Hence, travel time is not explicitly included in the cost function. The second term penalizes the deviation of the heading angle from the goal direction. The two terms are linearly combined using a relative weight w. Figure 11 illustrates components of the cost function.

Dynamic Optimizer

Many high efficiency optimization algorithms have been considered to enable real-time operation with MPC. Explicit methods move the computational burden offline and store the optimal control actions in a look-up table. The online computation effort can then be reduced to locating the measured initial state in the polyhedral partition and an affine function evaluation [24]. There are also fast MPC techniques such as move blocking, warm starting, or an early termination of an appropriate interior point method [25-27]. Such approaches will be considered in the future as necessary. In this study, as a first step to validate the problem formulation and the performance of defined constraints and cost function, as well as the performance of MPC with vehicle models of different fidelity, an exhaustive search is used as the dynamic optimizer.

The optimal control sequence that can minimize the cost function and satisfy the constraints is selected from a discrete steering command pool of $\left[-\delta_{\max}, -\delta_{\max}/2, 0, \delta_{\max}/2, \delta_{\max}\right]$, where $\delta_{\max}$ is determined based on Fig. 9. Starting from the initial state, the control commands from the pool are applied to the vehicle and the resulting trajectories are checked for constraint violation. If constraints are not satisfied, the search branch is terminated. Otherwise, next step prediction is performed by using the end state of last simulation as the initial state and applying all the steering commands from the pool. This process is repeated until a predetermined number of steps in the prediction horizon is reached. Once all the feasible steps are thus determined, their costs are evaluated and the control

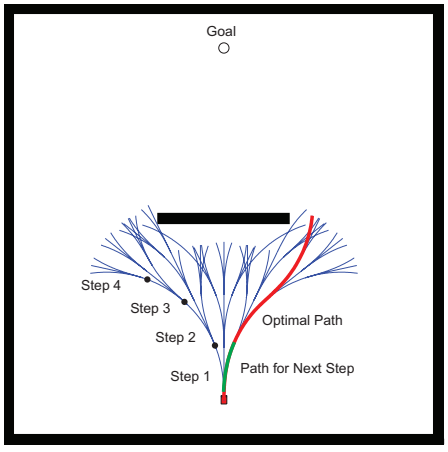

FIGURE 12. ILLUSTRATION OF THE EXHAUSTIVE SEARCH METHOD USING A STEERING COMMAND POOL OF THREE ELEMENTS

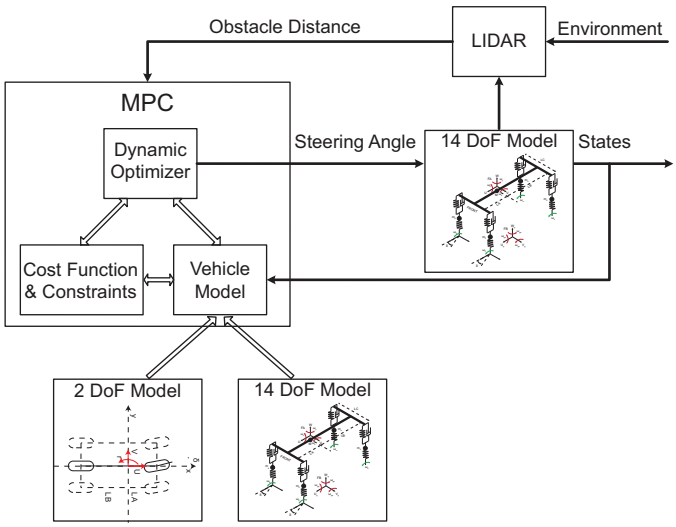

FIGURE 13. MPC-BASED HAZARD AVOIDANCE AS IMPLEMENTED IN THIS STUDY

sequence with minimum cost is considered as the optimal control sequence. The first element of this sequence is applied to the vehicle, and the process is iterated in the next simulation step. This idea is illustrated in Fig. 12 with a steering command pool of only three elements for clarity.

Prediction horizon and sampling time for the MPC are selected based on the speed of the vehicle, the minimum turning radius at that speed, and the detection range of the sensors to satisfy the following inequalities

$$\begin{aligned} U \cdot n \cdot T &\le D \\ \frac{\pi}{2} R_{\min} &\le U \cdot n \cdot T \\ R_{\min} + S &< D \end{aligned} \tag{1}$$

where U is the speed, D is the LIDAR detection range, R_{min} is the vehicle's minimum turning radius and S is the safety margin that accounts for the size of the vehicle. The first inequality simply states that the prediction horizon in terms of the traveled distance is limited by the sensor range. The second inequality ensures that the vehicle can make a 90° turn when necessary to avoid an obstacle. Finally, the last inequality ensures that there is enough distance between the vehicle and the obstacle during a 90° avoidance maneuver.

Figure 13 illustrates how Fig. 2 is customized for the purposes of this study.

SIMULATION RESULTS AND DISCUSSION

To validate the algorithm and study the effect of the complexity of the vehicle model used in the MPC, two simulation studies are conducted with two different obstacle maps. The speed of the vehicle, U, is fixed to be 20 m/s. The number of steps n in the prediction horizon is set to 4 steps. Using the inequalities (1), the sampling time T is set to

TABLE I. SIMULATION PARAMETERS

Parameter	Value	
	2 DoF	14 DoF
Vehicle speed, U	20 m/s	20 m/s
Prediction horizon length, n	4 steps	4 steps
LIDAR angular range	±90°	±90°
LIDAR angular resolution	0.1°	0.1°
Weighting parameter w	100	100
Maximum steering angle	2.8°	4.3°
Minimum turning radius	86.6 m	63.7 m
Planning sampling time, T	1.70 s	1.25 s
LIDAR detection range, D	136 m	100 m
Steering angle options	±2.8°, ±1.4°,0°	±4.3°, ±2.15°, 0°

1.25 s for the 14 DoF model and 1.70 s for the 2 DoF model. The LIDAR detection range D is then determined to be 100 m for the 14 DoF model and 136 m for the 2 DoF model. At each sampling cycle, the obstacle information is obtained from the LIDAR. A 2D LIDAR is assumed; i.e., the height of the obstacle is unknown. The LIDAR returns the distance between the vehicle and the closest obstacle boundaries in each radial direction at an angular resolution of 0.1°. The angular range is ±90° with the vehicle heading direction being the 0° direction. No noise or uncertainties are considered. Simulations are carried out using variable time step solvers (ode45 for the 2 DoF model, and ode23 for the 14 DoF model). Table I summarizes the parameters used in the simulation.

Several metrics are used to compare the performance of the system using the two different vehicle models in the MPC. One metric is the total time used to reach the target. This is proportional to the travel distance because the velocity of the vehicle is maintained constant. Another metric is the minimum distance to obstacles; a smaller minimum distance means the vehicle moves closer to the boundary of the obstacles. Other metrics include the maximum roll angle, maximum lateral acceleration, average roll angle, and average lateral acceleration. Table II summarizes the performance metrics and Figs. 14 and 15 compare the trajectories for the two maps considered.

The results with the 14 DoF model confirm that the presented formulation can successfully navigate the vehicle through the obstacle field to the target. For Map A, MPC with both the 2 DoF model and the 14 DoF model are successful in terms of avoiding the obstacles safely. When the 14 DoF model is used in the MPC, however, the algorithm performs better in terms of time to target and travel distance. This is due to the fact that MPC with the 14 DoF model uses a larger steering limit based on its capability to predict tire lift-off.

For Map B, MPC with 2 DoF model cannot avoid the obstacles due to its conservative steering limit derived from its range of validity. MPC with the 14 DoF model shows that it is actually possible to navigate through this obstacle field safely at the given speed when the vehicle is operated closer to its limits.

TABLE II. PERFORMANCE METRICS

	MAP A		MAP B	
	2 DoF	14 DoF	2 DoF	14 DoF
Time to target (s)	32.3	29.4	-	50.7
Travel distance (m)	641.2	582.2	-	1001.9
Min distance to obstacles (m)	8.46	6.43	-	14.4
Max roll angle (°)	1.59	2.11	-	2.12
Max lateral acceleration (g)	0.506	0.684	-	0.68
Avg roll angle (°)	1.21	1.34	-	1.33
Avg lateral acceleration (g)	0.390	0.442	-	0.43

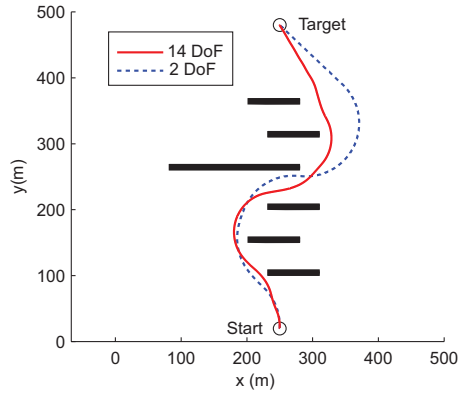

FIGURE 14. VEHICLE TRAJECTORIES FOR MAP A

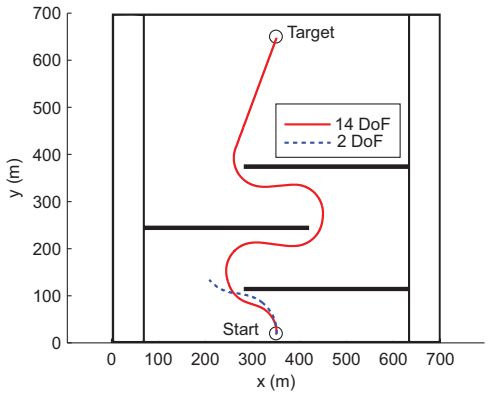

FIGURE 15. VEHICLE TRAJECTORIES FOR MAP B

It is very important to note that these results do not immediately lead to the conclusion that a 14 DoF model must be used in the MPC. The results only establish the importance of operating the vehicle close to its limits for better performance. In the results so far, the range of validity of the 2 DoF model has been used to determine the steering limits for that model, which prevented the MPC to push the vehicle to its limits. A different scenario is also conceivable in which the safety limits are established using the 14 DoF model, but the MPC still utilizes the 2 DoF model. The simulations for the two maps are repeated using this scenario and the results are summarized in Table III and Figs. 16 and 17.

These results show that when the safe steering limits are established using the 14 DoF model, the performance with the 2 DoF model can be very similar to the performance with the 14

TABLE III. PERFORMANCE METRICS WHEN 14 DOF MODEL'S STEERING LIMITS ARE USED FOR 2 DOF MODEL

	MAP A		MAP B	
	2 DoF	14 DoF	2 DoF	14 DoF
Time to target (s)	28.3	29.4	51.2	50.7
Travel distance (m)	559.9	582.2	1013.0	1001.9
Min distance to obstacles (m)	7.58	6.43	15.1	14.4
Max roll angle (°)	2.11	2.11	2.12	2.12
Max lateral acceleration (g)	0.684	0.684	0.68	0.68
Avg roll angle (°)	1.26	1.34	1.33	1.33
Avg lateral acceleration (g)	0.415	0.442	0.43	0.43

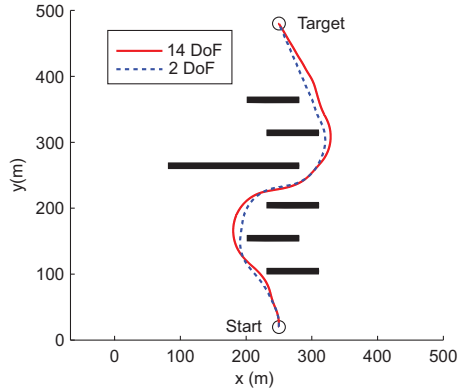

FIGURE 16. VEHICLE TRAJECTORIES FOR MAP A WHEN 14 DOF MODEL'S STEERING LIMITS ARE USED FOR 2 DOF MODEL

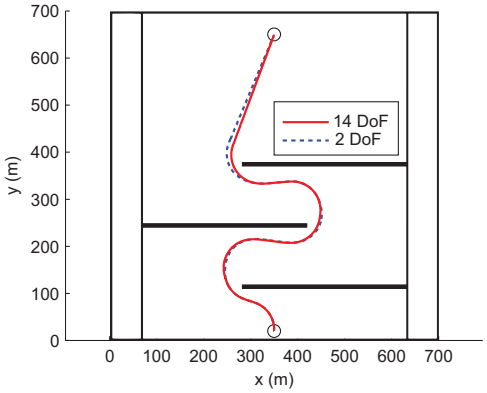

FIGURE 17. VEHICLE TRAJECTORIES FOR MAP B WHEN 14 DOF MODEL'S STEERING LIMITS ARE USED FOR 2 DOF MODEL

DoF model. For Map A, the 2 DoF model even outperforms the 14 DoF model in time to target. The comparable responses are likely due to basic idea of MPC that only the first steering command is implemented even if the prediction is made over several steps. The prediction errors of the 2 DoF model accumulate only with time; hence the predictions of the 2 DoF and the 14 DoF models are closer to each other in the beginning of the prediction horizon than at the end. In addition, since MPC is repeated at every time step, the predictions of the 2 DoF are corrected at each time step. Hence, 2 DoF model might be enough for the purposes of MPC under some conditions as

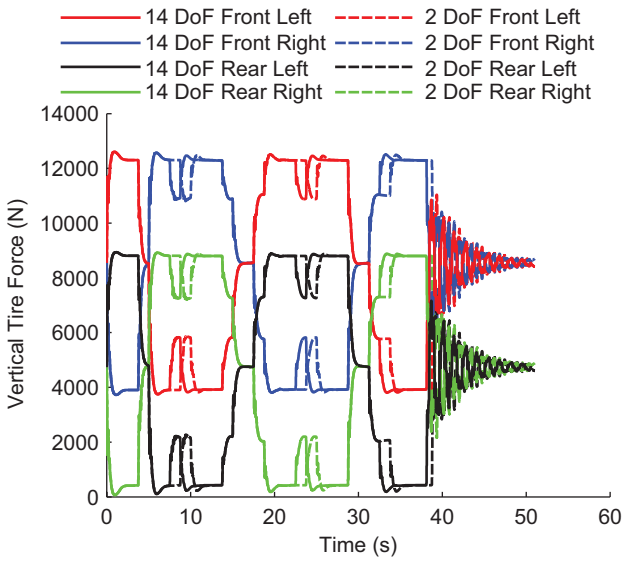

FIGURE 18. VERTICAL TIRE FORCES FOR MAP B WHEN 14 DOF MODEL'S STEERING LIMITS ARE USED FOR 2 DOF MODEL

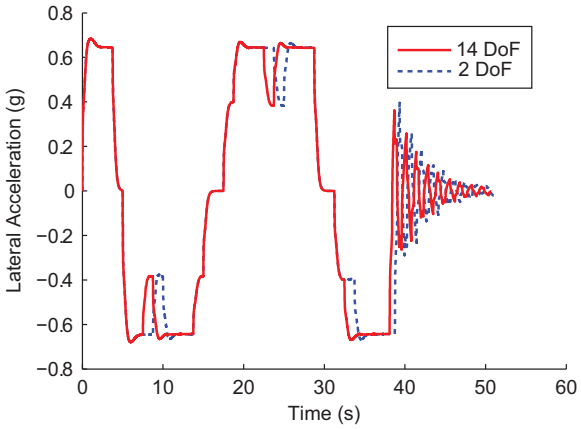

FIGURE 19. LATERAL ACCELERATIONS FOR MAP B WHEN 14 DOF MODEL'S STEERING LIMITS ARE USED FOR 2 DOF MODEL

long as the safe vehicle operation limits are established using a higher fidelity model.

For the second map, Figures 18 and 19 show the vertical tire forces and the lateral accelerations, respectively. From Fig. 18 it can be seen that the trajectories with both the 2 DoF and 14 DoF models are dynamically safe in terms of tire lift-off and are close to the boundary. Fig. 19 shows that the maximum lateral acceleration when the vehicle steers at 4.3° is approximately 0.65 g, which is larger than 0.5 g, the range of validity of the 2 DoF model. Nevertheless, the 2 DoF still performs well because of the abovementioned reasons.

This work has the following limitations. The vehicle speed is assumed to be constant and hence steering angle is considered as the only control input. Even though this reduces

the control input search space, it also potentially limits the performance of the algorithm. It also limits the obstacle fields that the UGV can go through safely without decelerating and accelerating. The 14 DoF employed in this study is certainly not the highest fidelity model available, but it was used in this paper as a first step towards higher fidelity models. Models derived using a multibody approach [28] can potentially improve the performance even further. It is also reasonable to expect an even better performance from higher fidelity models when uneven terrains, more realistic tire-terrain interactions, and uncertainties are included in the model. Finally, computational aspects of the algorithm need to be evaluated and solutions for a real-time implantation using high performance computing architectures need to be developed.

CONCLUSIONS

The paper presents the development of an MPC-based framework for hazard avoidance in large UGVs with significant vehicle dynamics. Unlike the existing MPC-based approaches, the framework uses only local information about the environment available from onboard sensors. The developed formulation is tested in simulation using a 14 DoF model of a typical 4 wheel truck as the vehicle platform and shows that the vehicle can navigate safely through two obstacle fields and reach the target.

The paper further investigates the effect of the fidelity of the model used in MPC on the performance of the hazard avoidance maneuver, where performance is characterized mainly by the time-to-target metric. Towards this end, two different models are used in the MPC; the 14 DoF model and a 2 DoF representation. The 2 DoF model is the typical choice in the literature for MPC and hence is used in this study as a benchmark. The results show that the 2 DoF does not give the best performance when the steering limits are based on the model's range of validity. Due to this conservative approach, the 2 DoF model may even fail to navigate the vehicle safely through an obstacle field that can actually be navigated safely with the 14 DoF model. However, the 2 DoF model can perform comparable to the 14 DoF model when the safe steering limits are derived from the 14 DoF model.

Hence, the conclusion is that higher fidelity models are needed for autonomous navigation to push the vehicle to its limits for best performance. However, that does not necessarily mean that the high fidelity model must be used within the MPC. A mixed-fidelity approach in which the safe operating limits are established using a higher fidelity model and the MPC is performed with a lower fidelity model may be adequate for satisfactory results. The right amount of fidelity that needs to be included in the MPC model is still subject to future research.

ACKNOWLEDGMENTS

This work was supported by the Automotive Research Center (ARC), a U.S. Army Center of Excellence in Modeling and Simulation of Ground Vehicles, led by the University of Michigan and U.S. Army TARDEC.

REFERENCES

[1] Vanderbilt, T., 2012, "Let the Robot Drive: The Autonomous Car of the Future Is Here", *WIRED*, available online: http://www.wired.com/magazine/2012/01/ff_autonomous cars/.

[2] Kerbrat, A., 2010, "Autonomous Platform Demonstrator", Report #21395, U.S. Army TARDEC, Warren,MI.

[3] Borenstein, J. and Koren, Y., 1991, "The Vector Field Histogram - Fast Obstacle Avoidance for Mobile Robots", IEEE Transactions on Robotics and Automation, **7**(3), pp. 278-288.

[4] Khatib, O., 1986, "Real-Time Obstacle Avoidance for Manipulators and Mobile Robots", International Journal of Robotics Research, **5**(1), pp. 90-98.

[5] Shimoda, S., Kuroda, Y., and Iagnemma, K., 2007, "High-Speed Navigation of Unmanned Ground Vehicles on Uneven Terrain Using Potential Fields", Robotica, **25**(4), pp. 409-424.

[6] Ulrich, I. and Borenstein, J., 1998, "VFH+: Reliable Obstacle Avoidance for Fast Mobile Robots", *Proceedings of IEEE International Conference on Robotics and Automation*, Leuven, Belgium, **2**, pp. 1572-1577.

[7] Ulrich, I. and Borenstein, J., 2000, "VFH*: Local Obstacle Avoidance with Look-Ahead Verification", *Proceedings of IEEE International Conference on Robotics and Automation*, San Francisco, CA, **3**, pp. 2505-2511.

[8] An, D. and Wang, H., 2004, "VPH: A New Laser Radar Based Obstacle Avoidance Method for Intelligent Mobile Robots", *Proceedings of World Congress on Intelligent Control and Automation*, Hangzhou, China, **5**, pp. 4681-4685.

[9] Gong, J., Duan, Y., Man, Y., and Xiong, G., 2007, "VPH+: An Enhanced Vector Polar Histogram Method for Mobile Robot Obstacle Avoidance", *Proceedings of IEEE International Conference on Mechatronics and Automation*, Harbin, China, pp. 2784-2788.

[10] Gong, J., Duan, Y., Liu, K., Chen, Y., Xiong, G., and Chen, H., 2009, "A Robust Multistrategy Unmanned Ground Vehicle Navigation Method Using Laser Radar", *Proceedings of IEEE Intelligent Vehicles Symposium*, Xi'an, China, pp. 417-424.

[11] Fox, D., Burgard, W., and Thrun, S., 1997, "Dynamic Window Approach to Collision Avoidance", IEEE Robotics and Automation Magazine, **4**(1), pp. 23-33.

[12] Ogren, P. and Leonard, N. E., 2005, "A Convergent Dynamic Window Approach to Obstacle Avoidance", IEEE Transactions on Robotics, **21**(2), pp. 188-195.

[13] Koren, Y. and Borenstein, J., 1991, "Potential Field Methods and Their Inherent Limitations for Mobile Robot Navigation", *Proceedings of IEEE International*

Conference on Robotics and Automation, Los Alamitos, CA, pp. 1398-1404.
[14] Tahirovic, A. and Magnani, G., 2011, "General Framework for Mobile Robot Navigation Using Passivity-Based MPC", IEEE Transactions on Automatic Control, **56**(1), pp. 184-190.
[15] Park, J. M., Kim, D. W., Yoon, Y. S., Kim, H. J., and Yi, K. S., 2009, "Obstacle Avoidance of Autonomous Vehicles Based on Model Predictive Control", Proceedings of the Institution of Mechanical Engineers, Part D: Journal of Automobile Engineering, **223**(12), pp. 1499-1516.
[16] Bevan, G. P., Gollee, H., and O'Reilly, J., 2010, "Trajectory Generation for Road Vehicle Obstacle Avoidance Using Convex Optimization", Proceedings of the Institution of Mechanical Engineers, Part D: Journal of Automobile Engineering, **224**(4), pp. 455-473.
[17] Gao, Y., Lin, T., Borrelli, F., Tseng, E., and Hrovat, D., 2010, "Predictive Control of Autonomous Ground Vehicles with Obstacle Avoidance on Slippery Roads", *Proceedings of ASME Dynamic Systems and Control Conference*, Cambridge, MA, **1**, pp. 265-272.
[18] Negrut, D., Tasora, A., Mazhar, H., Heyn, T., and Hahn, P., 2012, "Leveraging Parallel Computing in Multibody Dynamics", Multibody System Dynamics, **27**(1), pp. 95-117.
[19] Shim, T. and Ghike, C., 2007, "Understanding the Limitations of Different Vehicle Models for Roll Dynamics Studies", Vehicle System Dynamics, **45**(3), pp. 191-216.
[20] "Trucksim", 8.1 ed: Mechanical Simulation Corporation, 2012.
[21] Chen, B.-C. and Peng, H., 2005, "Rollover Warning for Articulated Heavy Vehicles Based on a Time-to-Rollover Metric", Journal of Dynamic Systems, Measurement and Control, **127**(3), pp. 406-414.
[22] Rakheja, S. and Piche, A., 1990, "Development of Directional Stability Criteria for an Early Warning Safety Device", SAE Transactions, **99**(2), pp. 877-889.
[23] Ervin, R., Winkler, C., Fancher, P., Hagan, M., Krishnaswami, V., Zhang, H., Bogard, S., and Karamihas, S., 1998, "Cooperative Agreement to Foster the Deployment of a Heavy Vehicle Htelligent Dynamic Stability Enhancement System", Report DTNH22-95-H-07002, University of Michigan Transportation Research Institute, Ann Arbor, MI.
[24] Hovland, S., Gravdahl, J. T., and Willcox, K. E., 2008, "Explicit Model Predictive Control for Large-Scale Systems Via Model Reduction", Journal of Guidance, Control, and Dynamics, **31**(4), pp. 918-926.
[25] Yildirim, E. A. and Wright, S. J., 2001, "Warm-Start Strategies in Interior-Point Methods for Linear Programming", SIAM Journal on Optimization, **12**(3), pp. 782-810.
[26] Cagienard, R., Grieder, P., Kerrigan, E. C., and Morari, M., 2007, "Move Blocking Strategies in Receding Horizon Control", Journal of Process Control, **17**(6), pp. 563-570.
[27] Wang, Y. and Boyd, S., 2010, "Fast Model Predictive Control Using Online Optimization", IEEE Transactions on Control Systems Technology, **18**(2), pp. 267-278.
[28] Blundell, M. and Harty, D., 2004, *The Multibody Systems Approach to Vehicle Dynamics*, Elsevier, New York, USA.